Thermochimica Acta 492 (2009) 101–109

Contents lists available at ScienceDirect

Thermochimica Acta

journal homepage: www.elsevier.com/locate/tca

Temperature dependence of the time constants for deconvolution of heat flow curves

Elena Moukhina*, Erwin Kaisersberger

Netzsch Geraetebau GmbH, Wittelsbacherstr. 42, Selb, Germany

ARTICLE INFO

Article history:
Available online 25 December 2008

Keywords:
DSC deconvolution
Time constant
Heat flow rate measurement
Temperature dependence

ABSTRACT

For the desmearing of the DSC signal the mathematical function for the description of the instrument response with its time constants is necessary. The temperature dependence of the time constant was found from DSC measurements for melting of metals, for empty crucibles, for the sensor without crucibles, and from LFA measurement for the crucible separate. The time constant decreases almost by a factor of two in the temperature range between −40 °C and 400 °C. The clear trend for the temperature dependence of the time constant was observed even at room temperature, where heat exchange by means of radiation is supposed to be zero. The mechanism, which dominates the heat transfer in the system, is found from the plot of the temperature dependence for the time constant. The heat loss to the surrounding gas and the thermal contact between sensor and crucible through the gas layer between are the main reasons for the temperature dependence of the time constant.

1. Introduction

Measurements carried out by the method of heat flux differential scanning calorimetry (DSC) contain information about the measured sample as well as instrument properties and measurement conditions. This dependence is shown in the smearing of the measured signal in comparison with the heat flow evolved or consumed by the sample. The degree of such smearing depends on the experimental conditions, heat capacity of the sample and properties of the measurement system [4]. As a result, the measured temperature at the maximum point of a melting peak shows a significant difference from the melting temperature of the metal sample, and the signal after complete melting, i.e. after the peak maximum, goes not immediately, but exponentially to the horizontal level. But it is known that after the maximum point of the DSC curve the sample is already molten and does not need any heat for its melting. As conclusion it is seen that the shape of measured peak does not correspond exactly to the heat consumed or evolving in the sample because of the thermal event. To get the correspondence between the curve shape and the heat processes in the sample, it is necessary to carry out the signal correction.

The correction of the signal peak, measured on the heat flux differential scanning calorimeter, consists of two parts [4]: temperature correction regarding the thermal resistance between sample and the point of the temperature measurement, and correction of the heat flow values by using of a deconvolution procedure regarding the system function of the instrument. By means of the deconvolution procedure the signal $f(t)$ corresponding to the true heat flow consumed or evolved in the sample because of thermal event in it, can be found from the measured DSC signal $F(t)$, and the known system function of the instrument $g(t)$ [1,2]:

$$F(t) = \int_0^t f(t')g(t - t')\ \mathrm{d}t' \tag{1}$$

Here the system function of instrument has the unit 1/s, because the integral of the system function over time must be equal to 1. To characterize the system function of the instrument usually one or several time constants are used. They correspond to the one or several different heat flow pathways in the system.

It is denoted, that time constants depend on the temperature, and the main reason for such dependence is the radiation in the heat exchange mechanism [5]. The sensitivity of the DSC instrument is also connected with its time constants, and the instrument sensitivity is investigated by [6]. Also here it is stated that high temperatures the main factor influencing the temperature dependence of the instrument sensitivity is the presence of radiation.

From another side it is known that the shape of the measured peaks for the same sample is different for the measurements carried out in different atmospheres. It means that the time constants depend on the gas nature in the measurement cell. Usually this is connected with the thin gas layer between crucible and sensor.

The purpose of the current work is to investigate the physical mechanisms influencing the temperature dependence of the time

* Corresponding author. Tel.: +49 9287881129; fax: +49 9287881144.
E-mail address: elena.moukhina@netzsch.com (E. Moukhina).

0040-6031/$ – see front matter © 2008 Elsevier B.V. All rights reserved.
doi:10.1016/j.tca.2008.12.022

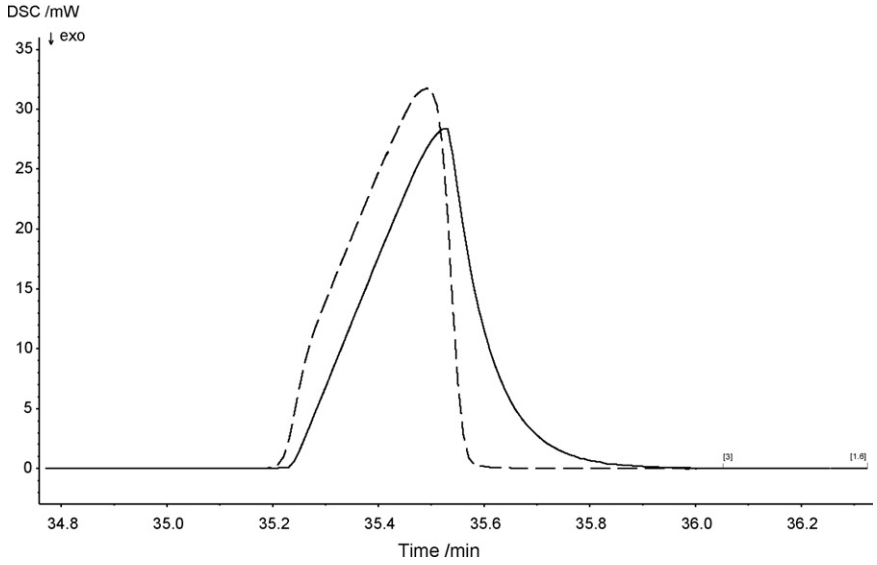

Fig. 1. Measured (solid) and corrected (dashed) curve shapes for Indium melting. Correction is done using system function with one time constant $g(t) = A\exp(-t/\tau)$.

constants for heat flux differential scanning calorimeters, and to find an answer for the contribution of these mechanisms.

2. Experimental

DSC measurements under the different conditions were carried out, and then the time constant (τ) was found from experimental data. For all experiments the deconvolution is done numerically according to algorithm described in [1] with system function $g(t) = A\exp(-t/\tau)$ with one time constant τ, A is the normalization factor. The time constant is the value in the system function, which leads to a fast return of the deconvoluted heat flow curve to the horizontal baseline after its peak maximum, when applied for correction of the measured curve.

2.1. Time constant from melting of metals at different temperatures

Measurements are done on the instrument NETZSCH DSC 204 F1, t-sensor, aluminum crucibles with pierced lid, mass 36 mg. Melting of the following metals from the standard calibration set: Hg, In, Sn, Bi, Zn. Sample masses from 11 to 13 mg, Hg: 32 mg, nitrogen atmosphere, heating rate 10 K/min. In Fig. 1 there is a typical example of the measured melting peak and the corrected peak. In Fig. 7a there is the temperature dependence of the time constant for this set of metals. For the temperature range between melting temperatures of Indium and Zinc the time constant changes monotonically from 4.4 to 2.6 s. The sensor and crucible heat capacity and the thermal conductivity show changes for this temperature range of several percent only and cannot be the reason for such big changes of the time constant.

2.2. Melting of indium in different atmospheres

Instrument NETZSCH DSC 204 F1, t-sensor, aluminum crucibles with pierced lid, sample mass 8.82 mg, gas flow 20 ml/min, heating rate 10 K/min, atmospheres: He, N_2, Ar, the results are presented in Fig. 2. The time constants are determined to 1.76, 3.75, 4.38 s, respectively, and they show a distinct dependence on the gas properties. For the heat exchange the thermal conductivity of gas can be

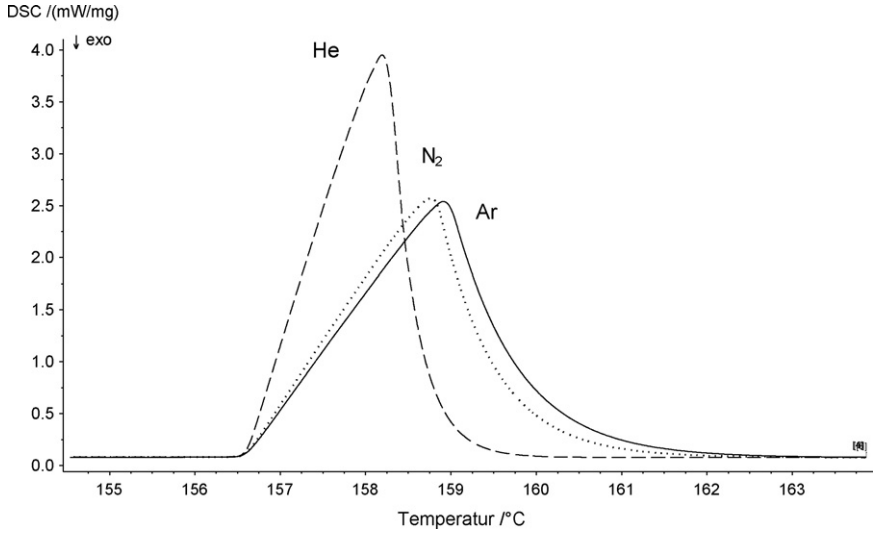

Fig. 2. Shape of the peak for In melting in atmospheres He (dashed), N_2 (dotted), Ar (solid), sample mass 8.82 mg, gas flow 20 ml/min, heating rate 10 K/min. Time constants are 1.76, 3.75 and 4.38 s correspondingly.

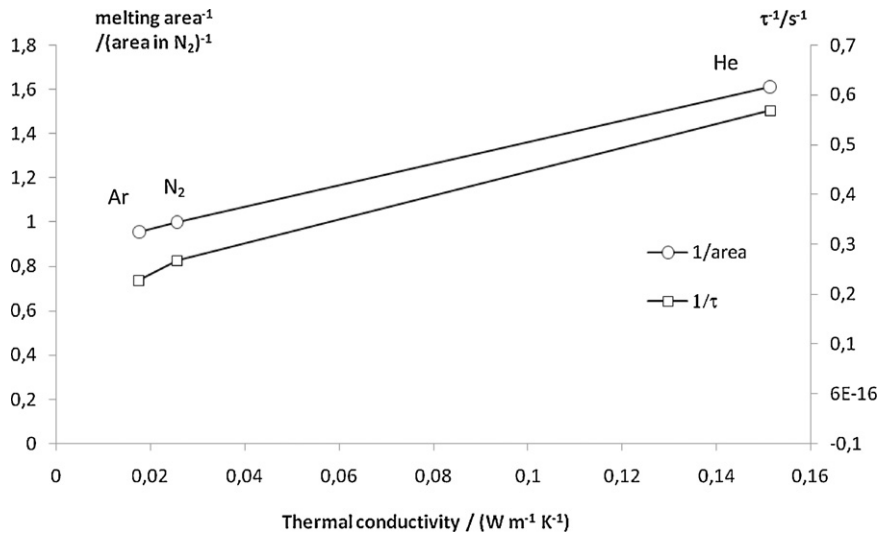

Fig. 3. Inverse time constant (squares) and inverse measured peak area (circles) for Indium melting peak in atmospheres Ar, N_2, He vs thermal conductivity of gas. Inverse peak area is shown normalized to the corresponding value in nitrogen. Linear dependence of these values on gas thermal conductivity corresponds to the case of convectional heat loss (line 4 in Table 1).

important. In Fig. 3 there is the inverse of the time constant and the inverse of measured peak area for the Indium melting peak in the atmospheres Ar, N_2, He plotted versus the thermal conductivity of the gases. The inverse peak area is shown relative to the corresponding value in Nitrogen. The different peak areas mean different values for instrument sensitivity. There is a distinct correlation between the instrument time constant and the gas properties. The dependence of the inverse sensitivity and the inverse time constant on thermal conductivity is close to a straight line but not direct proportional. In any case it could be confirmed that the sensitivity and time constant depend on the thermal conductivity of the surrounding gas.

2.3. Instrument response on light exposure: sensor with empty crucibles

Instrument: NETZSCH Photo DSC 204 F1, t-sensor, nitrogen atmosphere, aluminum crucibles without lids, crucible mass 22 mg. Isothermal conditions for temperatures between −50 °C and 200 °C with steps 25 °C. Under isothermal conditions the UV light beam came from the top side of the measurement cell to the opened sample crucible. Duration of the light impulse 5 s, diameter of the light beam is 2 mm. The system contains additional heat flow paths between sensor and crucibles including the influence of the thin gas layer, and heat flow from the crucibles to the surrounding gas. In Fig. 4 there are the typical measured and corrected curve shapes (exothermal) for isothermal measurements with light exposure. After correction regarding the time constant, the heat flow curve for the impulse is almost rectangular. For the measurements with exposure times 3, 5, and 10 s at the same temperature the time constant was independent from the light duration. However, the time constants presented in Fig. 7a show again a dependence on temperature, which cannot be explained by the temperature dependences of the heat capacity and thermal conductivity of the sensor and crucibles. It could be influence of the gas properties or of the radiation mechanism for the heat exchange.

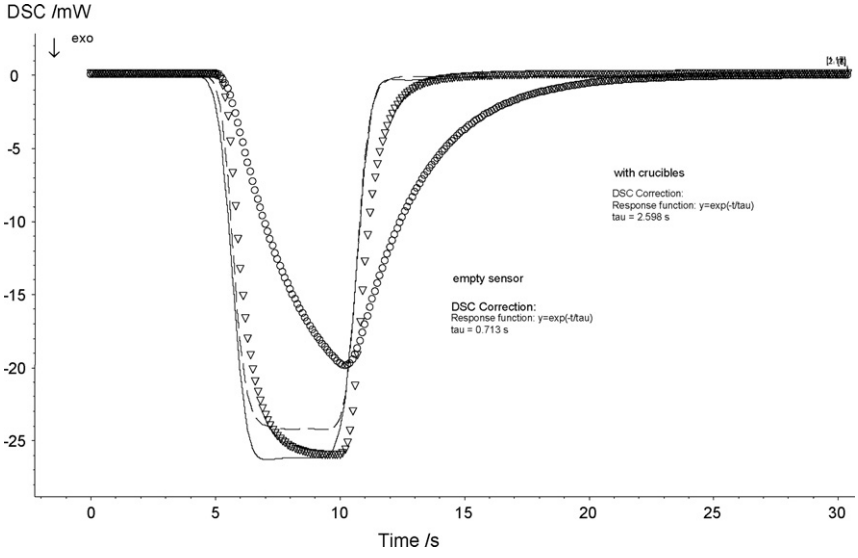

Fig. 4. Measured (circled) and corrected (dashed) curve shapes for isothermal measurement at 25 °C on NETZSCH Photo DSC 204 F1 instrument with two empty crucibles during light exposure. Measured (triangles) and corrected (solid) curve shapes for empty sensor for the same conditions. After correction regarding time constant the light impulse is shown almost rectangular. The time constant is independent from the light duration.

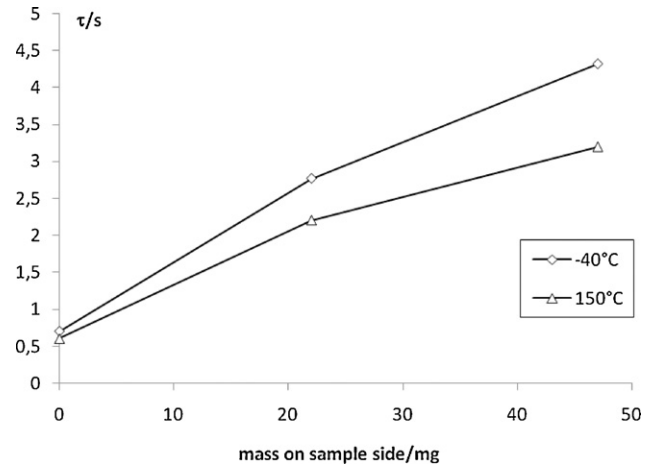

Fig. 5. Dependence of time constant on heat capacity; mass = 0 mean sensor without crucibles, m = 22 mg is the sensor with empty crucibles without lid, and m = 46 mg is the crucibles with lid and with sample inside.

2.4. Instrument response on light exposure: sensor without crucibles

The same instrument and measurement conditions as in the previous measurements were used. Here the time constant is measured without influence of the gas layer between the sensor and crucible. During this measurement the part of system time constant is found, which is coming from the sensor itself. It includes the heat transfer between furnace and sensor, the heat transfer inside the sensor between the sample position and the reference position and the heat transfer from the sensor to the gas. The time constant for the empty sensor is much less than for the sensor with empty crucibles. In Fig. 5 there are two DSC signals measured for the empty sensor and the sensor with crucibles and corrected curves for both signals. The same light impulse brings different measured peak areas for the measurement with crucible and without them. This difference in the total amount of heat received during lighting can be explained by the difference in the light absorption by the sensor and by the crucible material. In Fig. 7a there is the comparison of the time constants for the empty sensor and for the sensor with crucibles. The time constants for the empty sensor have weak dependence on temperature, whereas the time constants for the sensor with crucibles have clear temperature dependence. Reason could be the gas layer between sensor and crucible or heat loss due to convection to the surrounding gas.

2.5. Instrument response on light exposure: influence of thermal resistance between crucible and sensor

Isothermal experiments with UV light were done on the same instrument with different thermal resistances between crucible and sensor. For this purpose a thin round aluminum foil of thickness 0.1 mm with a diameter equal to the crucible diameter was used. For all experiments in this series the same crucible and the same foil were used to have the same summary mass of crucible and foil.

1. Foil inside crucible. One gas layer is between crucible and sensor. Area of gas layer is equal to bottom area of the crucible.
2. Foil is between sensor and crucible. Two gas layers are between crucible and sensor. Area of each gas layer is the same as before. Thermal resistance is twice higher as for previous experiment. The experimental time constant is now higher as before. At room temperature, for example, this doublicated thermal resistance results in an increase of the time constant from 2.97 to 3.43 s.
3. Part of this foil, which mass is 21% of the mass of full foil, is placed between sensor and crucible; the rest of the foil is placed inside the crucible. Now there are two gas layers between crucible and sensor, but the area of each of them is only 21% of the bottom area of the crucible. The thermal resistance is now (1/0.21) times higher than for the previous experiment and 9.5 times higher than for the first measurement. The experimental time constant is higher than in the two previous experiments. At room temperature, for example, such increasing of the thermal resistance results in an increase of the time constant from 2.97 to 4.33 s.

The experimental results for time constant for temperatures between 30 °C and 200 °C are shown in Fig. 7b.

2.6. Separate crucible without sensor

The heat transfer inside an aluminum crucible and the heat loss from it to the surrounding gas are measured outside of the DSC instrument. For such a purpose the laser flash method can be used. This experiment was carried out on the NETZSCH LFA 447 for isothermal conditions from 25 °C to 300 °C in step of 25 °C in air. The functional scheme of laser flash instruments can be found, for example, in [7]. The short light pulse comes to the bottom side of the measured object, the heat is absorbed by the bottom surface, and the infrared sensor indicates the temperature increase on the top side of the measured object. In the current case the Xenon lamp had a light duration 0.18 ms. From the recorded curve shape the thermal diffusivity, radiation, and heat loss due to convection can be found. The crucible is placed on the orifice in the support, which diameter is a little higher than the crucible bottom diameter, and

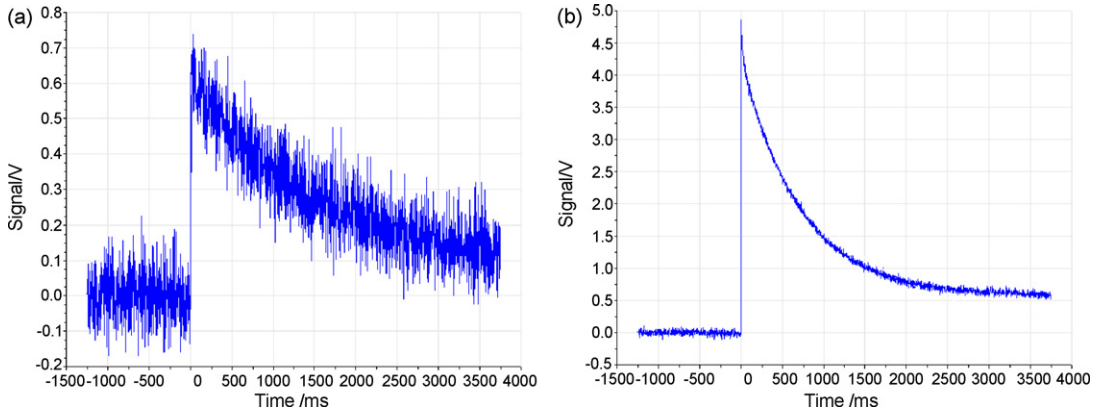

Fig. 6. Typical signal for temperature behavior measured for separate aluminum crucible in LFA447 after it got the heat from Xenon flash lamp for 25 °C (a) and 300 °C (b).

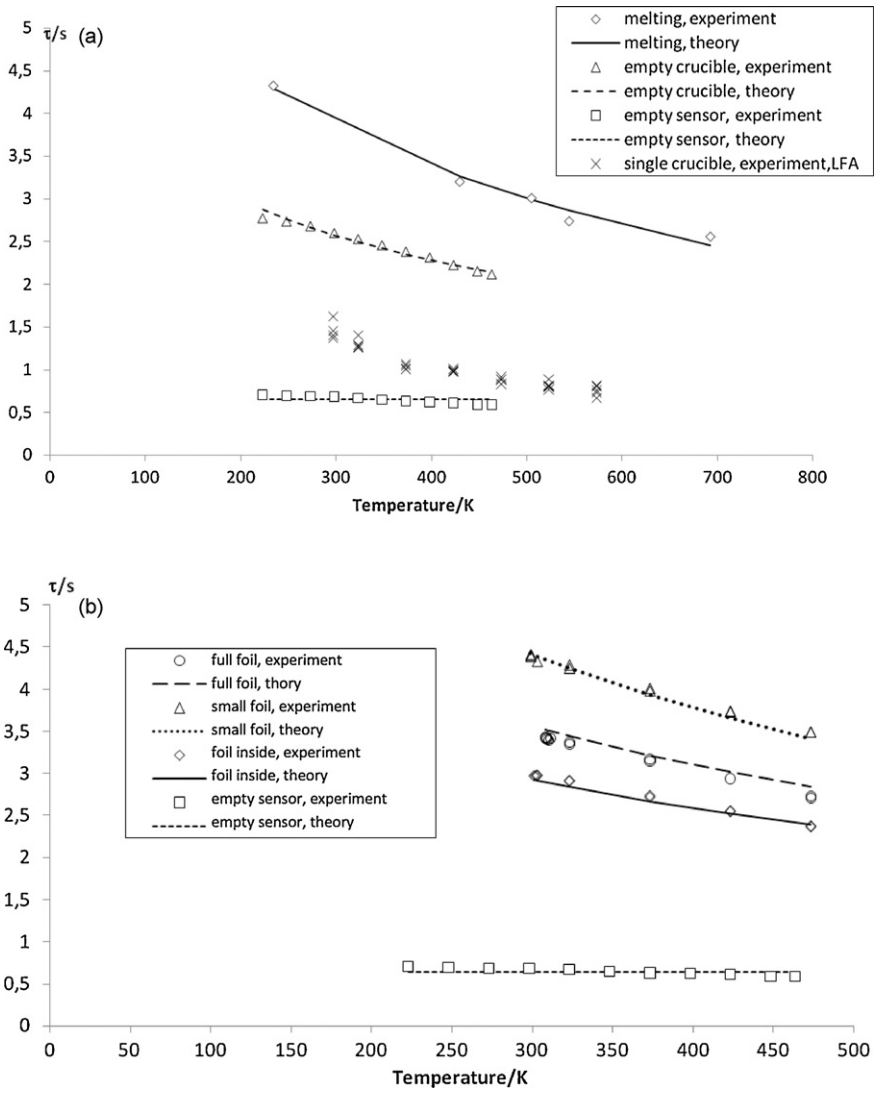

Fig. 7. (a) Experimental (data points) and calculated (curves) results. Experimental time constant found from melting peaks of metals Hg, In, Sn, Bi, Zn (diamonds) in crucibles with lids. Time constant for empty sensor (squares) has weak dependence on the temperature, whereas sensor with crucibles without lids (triangles) has clear dependence on the temperature. Measured time constant for the single crucible (crosses) has clear temperature dependence. Even values for 25 °C and 50 °C show the difference. All theoretical curves are calculated for DSC data according to formula (11) with $C_s = 0$ for empty sensor, $C_s = 0.020$ J/K for empty crucible and $C_s = 0.034$ J/K for melting experiments. (b) Experimental (data points) and calculated (curves) results for different thermal resistances between sensor and crucible. Experimental time constant found for empty sensor (squares), crucible with aluminium foil inside (diamonds), full foil between sensor and crucible (circles) and small foil between sensor and crucible (triangles). All theoretical curves are calculated for DSC data according to formula (11) with $C_s = 0.023$ J/K. This experiment is used for exact determination of the contribution of the gas layer and contribution of convection into temperature dependence of time constant.

contact area between the crucible and its support is very small. The measurement time was 4 s. In Fig. 6 there is the typical signal for the temperature behavior measured for a single aluminum crucible in such an experiment. After relaxation, the signal comes not to the same temperature as it was before the shot, but to a slightly higher temperature, because the system has got some heat. The reason of the temperature decrease is the heat loss to the surrounding gas, because the edge between the crucible and the support is very small and cannot be compared with the area of contact present at DSC measurements. The temperature dependence of the time constant is shown in Fig. 7a. The time constant in this temperature range changes from 1.464 to 0.755 s and this changes can be explained only by the heat loss from the crucible to the surrounding.

3. Modeling and calculation of the system time constant

The calculation of the time constants was based on the scheme shown in Fig. 10a. The system consists of the furnace with the furnace temperature T_f, the sensor with sensor temperature at the sample position T_{ss} and sensor heat capacity at the sample position C_{ss}, the sample with heat capacity C_s and temperature T_s; the sensor temperature at the reference position T_{sr}, sensor heat capacity at the reference position C_{sr}, reference with heat capacity C_r and temperature T_r. The contact between sample and sample crucible is not taken into account; it was assumed that the sample has the same temperature as the sample crucible, and the used sample heat capacity C_s has the meaning of heat capacity of sample with sample crucible. The furnace has direct contact to the sensor. The effects of radiation heat transfer and influence of gas properties are taken into account in the current consideration with gas temperature T_{gas}, thermal resistance between sample (or reference) to gas R_g, emissivity for furnace K_f and for sample and reference K_s and K_r, respectively. The thin gas layer between sensor and reference crucible and between sensor and sample crucible is taken into account in the values R_r and R_s. If the thermal contact between crucible and sensor is the thin gas layer, then the corresponding thermal resistance depends on the temperature inverse to thermal conductivity of gas λ_{gas}. The thermal resistance between sample (or reference)

Table 1
Limiting cases for time constants and sensitivity values as function of temperature.

	Description	General dependence τ on temperature	Temperature dependence for τ with $R_s = a/\sqrt{T}$, $R_g = b/\sqrt{T}$, $R_{rad} = 1/(4K\sigma T^3)$	Sensitivity for steady-state heating: (a) general formula; (b) temperature dependence
1	Empty sensor, no crucibles $R_s \to 0$, $C_s \to 0$ no radiation $R_{rad} \to \infty$, no convection heat loss $R_g \to \infty$	$\tau = C_{ss}R_f$	–	0
2	Sensor with two crucibles, no gas between sensor and crucibles $R_s \to 0$, no radiation $R_{rad} \to \infty$, no convection heat loss $R_{rad} \to \infty$	$\tau = (C_s + C_{ss})R_f$	–	R_f
3	Sensor with two crucibles, gas layer between sensor and crucibles no radiation $R_{rad} \to \infty$, no convection heat loss $R_g \to \infty$	$\tau = C_{ss}R_f + C_s(R_s + R_f)$, τ is linear to $1/\lambda_{gas}$	$\tau = R_f(C_s + C_{ss}) + aC_s/\sqrt{T}$	R_f
4	Sensor with two crucibles, convectional heat loss, no gas between sensor and crucibles $R_s \to 0$, no radiation $R_{rad} \to \infty$	$\tau = \frac{(C_s+C_{ss})R_fR_g}{R_f+R_g}$, $1/\tau$ is linear to λ_{gas}	$\tau = \frac{(C_s+C_{ss})R_fb}{b+R_f\sqrt{T}}$	(a) $\frac{R_fR_g}{R_f+R_g}$, (b) $\frac{b}{b+R_f\sqrt{T}}$
5	Sensor with two crucibles, gas layer between sensor and crucibles, convectional heat loss no radiation $R_{rad} \to \infty$	$\tau = \frac{C_sR_g(R_s+R_f)+C_{ss}R_f(R_s+R_g)}{R_s+R_f+R_g}$	$\tau = \frac{(bC_s+aC_{ss}+bC_{ss})R_f+abC_s/\sqrt{T}}{a+b+R_f\sqrt{T}}$	(a) $\frac{R_fR_g}{R_s+R_f+R_g}$, (b) $\frac{bR_f}{a+b+R_f\sqrt{T}}$
6	Sensor with two crucibles, radiation no gas between sensor and crucibles $R_s \to 0$, no convection heat loss $R_g \to \infty$	$\tau = \frac{(C_s+C_{ss})R_fR_{rad}}{R_f+R_{rad}}$, $1/\tau$ is linear to T^3	$\tau = \frac{(C_s+C_{ss})R_f}{1+4K\sigma R_fT^3}$	(a) $\frac{R_fR_{rad}}{R_f+R_{rad}}$, (b) $\frac{R_f}{1+4K\sigma R_fT^3}$
7	Sensor with two crucibles, radiation, layer between sensor and crucibles, convectional heat loss	Formula in text	$\tau = \frac{aC_{ss}R_f+b(C_s(R_f+a/\sqrt{T})+C_{ss}R_f(1+4aK\sigma T^{5/2}))}{a+b+R_f\sqrt{T}+4abK\sigma T^{5/2}+4bK\sigma T^3}$	(a) $\frac{R_fR_gR_{rad}}{(R_gR_{rad}+R_s(R_g+R_{rad})+R_f(R_g+R_{rad})}$, (b) $\frac{R_fb}{a+b+R_f\sqrt{T}+4abK\sigma T^{5/2}+4bK\sigma T^3}$
8	Empty crucible in gas with radiation, $C_s\frac{dT_s}{dt} = -\frac{T_s-T_{gas}}{R_g} + K\sigma T_f^4 - K\sigma T_s^4$	$\tau = \frac{C_sR_gR_{rad}}{R_g+R_{rad}}$, $1/\tau$ is linear to λ_{gas} and T^3	$\tau = \frac{bC_s}{\sqrt{T}+4K\sigma bT^3}$	–

and surrounding gas is also inverse to thermal conductivity of gas λ_{gas}. The dependence of gas thermal conductivity on temperature is known [3] and in the first approximation is proportional to the square root of the absolute temperature: $\lambda_{gas} = k\sqrt{T}$.

The full system for describing of the heat transfer can be written in the following form:

$$C_r\frac{dT_r}{dt} = \frac{T_{sr}-T_r}{R_r} - \frac{T_r-T_{gas}}{R_g} + K_r\sigma T_f^4 - K_r\sigma T_r^4$$
$$C_s\frac{dT_s}{dt} = \frac{T_{ss}-T_s}{R_s} - \frac{T_s-T_{gas}}{R_g} + K_s\sigma T_f^4 - K_s\sigma T_s^4$$
$$C_{sr}\frac{dT_{sr}}{dt} = \frac{T_f-T_{sr}}{R_{sr}} - \frac{T_{sr}-T_r}{R_r}$$
$$C_{ss}\frac{dT_{ss}}{dt} = \frac{T_f-T_{ss}}{R_{ss}} - \frac{T_{ss}-T_s}{R_s} \quad (2)$$

This system of equations can be solved for the following initial conditions: the temperature of furnace, gas, reference and sensor is equal to T_{iso}, initial sample temperature differs from it by the value T_0. The solution with these initial conditions means the relaxation of the sample temperature to the equilibrium system temperature T_{iso}. Initial conditions:

$$T_s(0) = T_{iso} + T_0, \quad T_{ss}(0) = T_{iso}, \quad T_{sr}(0) = T_{iso},$$
$$T_r(0) = T_{iso}, \quad T_{gas}(t) = T_{iso}, \quad T_f(t) = T_{iso} \quad (3)$$

For the symmetric sensor $R_{ss} = R_{sr}$ and denoted as R_f. If the thermal contact between furnace and sensor is much better then inside the sensor between sample position and reference position, then the system of four equations splits into two independent parts for sample and reference, and the reference part has constant temperature whereas the sample part has temperature relaxation. Because of the direct contact between furnace and sensor no big temperature difference between furnace and measurement system exists, therefore the following series can be used:

$$T_r^4 \approx T_f^4 + 4T_f^3(T_r - T_f) \quad (4)$$

$$T_s^4 \approx T_f^4 + 4T_f^3(T_s - T_f) \quad (5)$$

After this simplification for radiation, the radiation thermal resistance $R_{rad} = 1/(4K\sigma T^3)$ can be introduced and the scheme of the heat exchange can be presented as the electric circuit analogue in Fig. 10b. The measured signal is the temperature difference between two points on the sensor, caused by heat flow differences:

$$T_{ss}(t) - T_{sr}(t) = \frac{-C_sR_fR_gR_{rad}T_0}{\sqrt{A_0^2 - 4C_sC_{ss}R_sR_fR_{rad}R_gR_0}} \times \left(\exp\left(-\frac{A_0 - \sqrt{A_0^2 - 4C_sC_{ss}R_sR_fR_{rad}R_gR_0}}{2C_sC_{ss}R_sR_fR_{rad}R_g}t\right) + \exp\left(-\frac{A_0 + \sqrt{A_0^2 - 4C_sC_{ss}R_sR_fR_{rad}R_gR_0}}{2C_sC_{ss}R_sR_fR_{rad}R_g}t\right)\right) \quad (6)$$

where

$$A_0 = C_s(R_s + R_f)R_gR_{rad} + C_{ss}R_f(R_gR_{rad} + R_s(R_g + R_{rad})) \quad (7)$$

$$R_0 = R_gR_{rad} + R_s(R_g + R_{rad}) + R_f(R_g + R_{rad}) \quad (8)$$

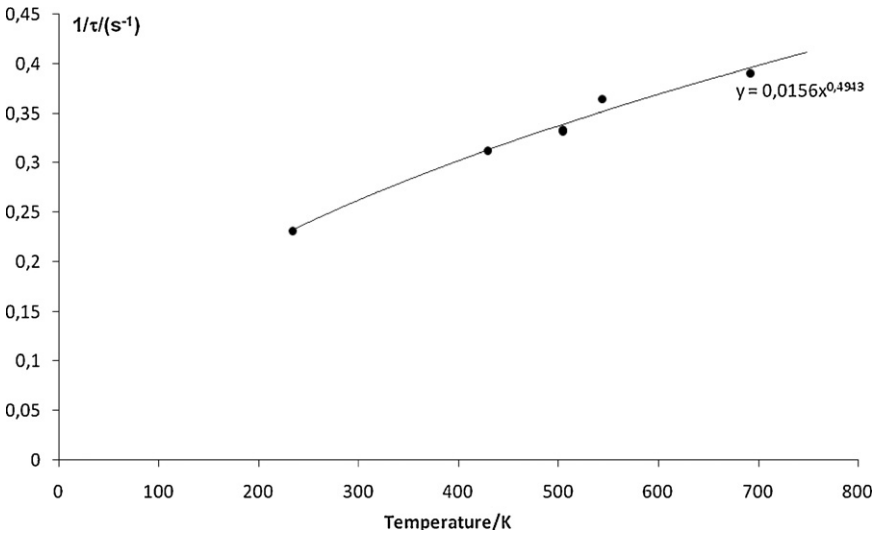

Fig. 8. Inverse time constant for metal melting with power function as trend line. The degree of power is very far from the value 3 (describing heat radiation mechanism) and close to value describing the influence of gas.

$R_{rad} = 1/(4K_r\sigma T_f^3)$ is the thermal resistance for radiation heat exchange.

σ is Stephan–Boltzman constant, K_r is the emissivity multiplied by area of reference crucible.

In our interest is only the maximal time constant:

$$\tau = \frac{2C_sC_{ss}R_sR_fR_{rad}R_g}{A_0 - \sqrt{A_0^2 - 4C_sC_{ss}R_sR_fR_{rad}R_gR_0}} \quad (9)$$

If one of the values R_s, R_f, R_{rad}, R_g is much less then another value from this set, then it means that one of the heat exchange mechanisms prevails over others, and then the following series can be used:

$$\sqrt{1 - \frac{4C_sC_{ss}R_0R_sR_fR_gR_{rad}}{A_0^2}} \approx 1 - \frac{2C_sC_{ss}R_0R_sR_fR_gR_{rad}}{A_0^2} \quad (10)$$

Then have the maximal time constant $\tau = A_0/R_0$ for the sensor with two crucibles with gas layer between sensor and crucibles, convectional heat loss and radiation exchange between crucibles and furnace:

$$\tau = \frac{C_sR_gR_{rad}(R_s + R_f) + C_{ss}R_f(R_gR_{rad} + R_s(R_g + R_{rad}))}{R_gR_{rad} + R_s(R_g + R_{rad}) + R_f(R_g + R_{rad})} \quad (11)$$

Calculation results are graphically presented in Fig. 7a and b by lines. All theoretical curves are calculated for DSC data according to formula (11) with heat capacities $C_s = 0$ for empty sensor, $C_s = 0.020$ J/K for empty crucible without lid, $C_s = 0.024$ J/K for crucible with foil and $C_s = 0.034$ J/K for melting experiments. For the measurements with different thermal resistances the values 2 and 9.5 are used for the ratio between actual thermal resistance and thermal resistance for measurement with the aluminum foil inside the crucible. Other values were found from the best fit of formula (11) with experimental DSC data.

The same equation system solved for furnace heating with the constant heating rate β and for a symmetric sensor gives the temperature difference $T_{ss}(t) - T_{sr}(t)$ after a relaxation time $t \gg \tau$:

$$T_{sr}(t) - T_{ss}(t) = \mathrm{Sens}(C_s - C_r)\beta \quad (12)$$

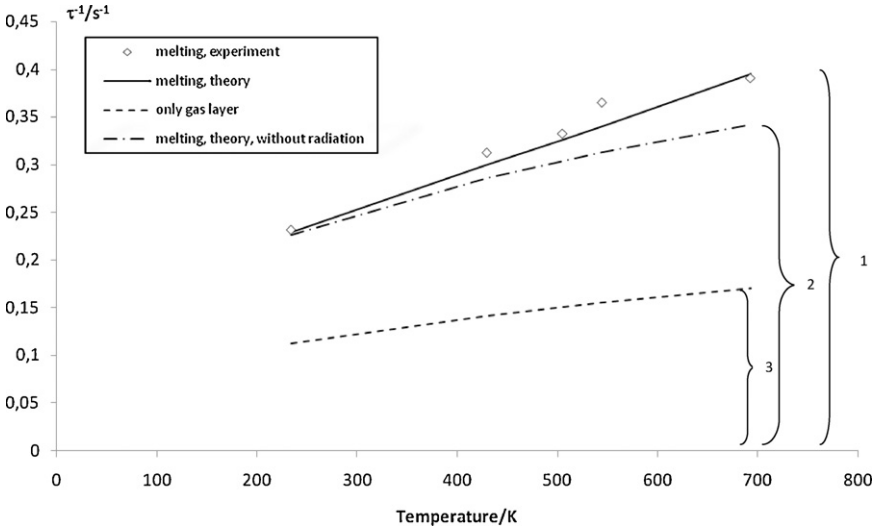

Fig. 9. Inverse of the experimental (diamonds) time constant for metal melting with calculated curves according to formula (11) (solid line, 1), calculation for model without radiation effect is done by the same formula for $K = 0$ (solid-dashed, 2) and for the model with only gas layer heat exchange(dashed, 3), where $K = 0$, $b \to \infty$. The theoretical model allows to find the influence of each mechanism to the time constant.

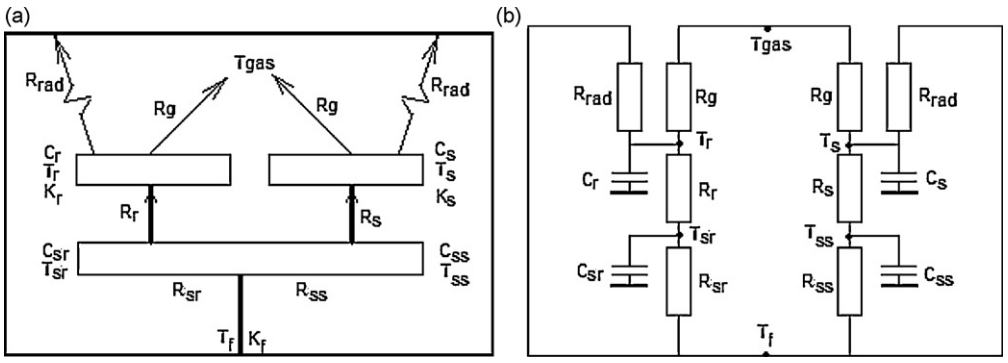

Fig. 10. Scheme of heat exchange for calculation of the time constant (a) and electrical model circuit (b) after simplification according formula ((4) and (5)).

where Sens is the sensitivity of the system:

$$\text{Sens} = \frac{R_f R_g R_{rad}}{R_g R_{rad} + R_s(R_g + R_{rad}) + R_f(R_g + R_{rad})} \quad (13)$$

The temperature dependence of the time constant and of the sensitivity for limiting cases from it can be found in Table 1.

For the solving of differential equations the software Mathematica 6.0 was used.

4. Discussion

All experimental results are presented in Fig. 7a and b. The temperature dependence of the time constants for empty sensor shows very slight decreasing trend with increasing temperature, no big influence from gas conductivity or from radiation heat loss is present. However, all other experimental results with the presence of crucibles show a very clear decreasing of the time constant with increasing temperature. The first assumption for the reason of such decreasing is the heat loss due to radiation, because radiation mechanism has the strongest dependence on the temperature. If only radiation heat loss is present then according to calculation the inverse time constant should have cubic dependence on temperature (T^3, see line 6 in Table 1). However the inverse time constant from the measured peaks has the exponent for the temperature dependence very far from 3: see Fig. 8. Of course, this degree does not take into account the thermal conductivity of the sensor itself, but it allows saying that the main mechanism responsible for the temperature dependence of the time constant and for the heat exchange at temperatures up to 700 K is not heat radiation. Exact calculation of time constant according formula (11) for a process with and without radiation heat exchange shows that for the current case the contribution of radiation to time dependence is very small (Fig. 9).

Another influence on the temperature dependence of the time constant is based on the thermal conductivity of the gas. The influence of the gas properties on the heat exchange can be seen in the difference of the measured peak shape for Indium melting in different gases (Fig. 2). Here could be two reasons of such influence: the first reason is that the thermal resistance of a thin gas layer between sensor and crucible depends on temperature because of gas thermal conductivity, The second reason could be convectional heat loss from the crucibles to the surrounding gas (Fig. 10).

The influence of gas layer is confirmed experimentally by the measurements with the different thermal resistance. But here increasing of the thermal resistance by 9.5 times results in an increase of the time constant from 2.97 to 4.33 s, which is only 1.46 times.

The experimental confirmation of convection is seen in the measurement of heat loss from a separate crucible by the LFA method, where temperature dependence of its time constant is detectable even between temperatures 25 °C and 50 °C and almost no contact area between crucible and support is present.

Another confirmation of the presence of convectional heat loss comes from the measurements in the different gases. If the measured peak area for Indium melting in Nitrogen is 100% then the measured area in argon is 104% and in He only 62%, if the same sensitivity calibration is used. According to the formula from Table 1, the temperature dependence of the sensitivity cannot be detected if gas influence comes only from the gas layer between sensor and crucible (see line 3 in the last column).

The theoretical model (11) allows to fit the time constants from all DSC experiments with the known heat capacity of the crucible including a sample for each measurement, with known ratio of contact resistance between sensor and crucible for experiments with different thermal resistance, and with one set of other parameters for the fit of all DSC experiments. The measurements with different thermal resistances allow to determine exactly, what is the contribution of the gas layer to temperature dependence of time constant, and what is the contribution of convection. The theoretical model allows to find the influence of each mechanism to the time constant. The calculation of inverse time constant with the same parameters is done here for the model with all three mechanisms of heat exchange (solid line in Fig. 9), for the model without radiation effect, which includes gas layer and convection (Fig. 9, dot-and-dash line), and for the model with only a gas layer heat exchange (Fig. 9, dashed line). Therefore it can be concluded that the mechanism for the heat loss to the surrounding gas by convection is one of the main reasons for the temperature dependence of the sensitivity; this mechanism exists in the DSC systems in the measured temperature range and cannot be neglected.

5. Conclusions

- Differences between measured areas for melting peaks in different gases indicate the heat loss from the crucibles to the surrounding gas.
- The inverse of the time constants show a dependence on temperature even for the lower temperatures nearly proportional to the square root of the absolute temperature; this indicates two comparable heat flow paths: the heat loss to the surrounding gas and the heat transport through the gas layer between sensor and crucible.
- The inverse of the time constants show a linear dependence on the thermal conductivity of the gas and this is interpreted as heat loss to the surrounding gas.

- The heat loss of the separate crucible shows a temperature dependence and this is connected with the heat loss to the surrounding gas.
- The main influence on the time constant at low temperatures comes from the thermal conductivity of the gas and its dependence on temperature.
- The time constant which is found at a specific temperature, may not be used for deconvolution of data, measured at other temperatures, even if the difference would be only 25 °C.

References

[1] H.J. Flammersheim, N. Eckhardt, W. Kunze, Thermochim. Acta 187 (1991) 269.
[2] H.J. Flammersheim, N. Eckhardt, G. Rudakoff, Wiss. Beitrage FSU Jena, Therm. Analysenverfahren Industrie Forschung 4 (1990) 62.
[3] E.W. Lemmon, R.T. Jacobsen, Int. J. Thermophys. 25 (2004) 21.
[4] G. Höhne, W. Hemminger, H.-J. Flammersheim, Differential Scanning Calorimetry, Springer, 1995.
[5] W. Baumann, et al., Thermochim. Acta 472 (2008) 50–54.
[6] V.A. Drebushchak, J. Ther. Anal. Calorim. 76 (2004) 941–947.
[7] S. Min, J. Blumm, A. Lindemann, Thermochim. Acta 455 (2007) 26–29.